RICE UNIVERSITY

Optimization of the Proteasomal Degradation Reporter (*e*Deg-On) System for CRISPR-mediated Whole-genome Knockout Screens

by

Yiwen Liu

A THESIS SUBMITTED
IN PARTIAL FULFILLMENT OF THE
REQUIREMENTS FOR THE DEGREE

Master of Arts

APPROVED, THESIS COMMITTEE

Laura Segatori, Thesis Advisor
Associate Professor, Department of
Chemical and Biomolecular Engineering

Weiwei Zhong
Assistant Professor, Department of
BioSciences

Yousif Shamoo
Professor, Vice Provost for Research,
Department of BioSciences

Daniel Wagner
Associate Professor, Department of
BioSciences

HOUSTON, TEXAS
April 2017

ABSTRACT

Optimization of the Proteasomal Degradation Reporter (*e*Deg-On) System for CRISPR-mediated Whole-genome Knockout Screens

by

Yiwen Liu

Protein folding and clearance of misfolded proteins are crucial to maintain cellular homeostasis (Jariel-Encontre et al., 2008). Misfolded proteins may associate with other cellular components and possibly impair their functions. They may also self-associate to form insoluble aggregates, which are the hallmarks of a number of neurodegenerative diseases, such as Parkinson's (Olanow and McNaught, 2006) and Alzheimer's (Oddo, 2008). The ubiquitin proteasome system (UPS) is the main pathway that catalyzes the degradation of soluble misfolded proteins in mammalian cells. Therefore, enhancing the UPS activity through activation of proteasomal degradation is considered a promising strategy to ameliorate phenotypes associated with the accumulation of misfolded proteins. Modulation of specific UPS components, for instance, results in increased degradation of target proteins (Rechsteiner and Hill, 2005 and Vilchez et al., 2012). However, our current understanding of the molecular mechanism underlying proteasomal degradation is still limited, limiting the rational design of pharmacologic strategies to enhance UPS activity. As a result, proteasome activators are rare and remain poorly characterized (Huang and Chen, 2009).

To overcome these limitations, researchers in my group developed a cell-based platform (the *e*Deg-On system) to monitor changes in UPS activity. This genetic circuit links increase in UPS activity to an increase in fluorescent output, thereby providing a reliable tool for the discovery of proteasome activators. The CRISPR-cas technology has emerged as powerful technique to introduce genetic modifications at the whole-genome scale. I optimized the *e*Deg-On system and evaluated it for pooled screening of whole-genome CRISPR-mediated knockout library. I replaced the antibiotic resistance gene in the *e*Deg-On system and assessed the response of HEK293 cells stably expressing the *e*Deg-On system to modulation of proteasomal degradation. To evaluate the use of a stable cell line expressing the *e*Deg-On system as a reporter assay in the context of a pooled CRISPR-mediated screen, I conducted mock screens using different ratios of positive and negative controls. The results obtained demonstrate that the *e*Deg-On system can be used as a reporter assay for CRISPR-mediated whole-genome knockout screens.

The use of the *e*Deg-On system to conduct genetic screen for the discovery of molecules that function as proteasome regulators will contribute to the development of therapeutic strategies for protein misfolding diseases. Further applications of this study include targeting the UPS function for therapeutic applications as well as for enhancing the production of recombinant proteins in industrial settings.

Acknowledgments

First of all, I would like to express my gratitude to my advisor, Dr. Laura Segatori, for her support throughout my entire journey of thesis work. I am deeply indebted to her help and guidance during these years, and I am very grateful for the lessons she taught me about persistence, endurance, creativity and independence.

I would also like to thank my colleagues in the Segatori lab. They have always been very helpful, and I cherish the days of pains and gains we experienced together in lab and in life.

I would also like to give special thanks to my committee members, Dr. Weiwei Zhong, Dr. Yousif Shamoo and Dr. Daniel Wagner, for their guidance and suggestions through the years.

I could not be more grateful to my parents and my family. It is their words and support that allows me to pursue my dream across the globe.

Contents

List of Figures

List of Tables

Chapter 1

Introduction

The ubiquitin proteasome system (UPS) plays an important role in degrading misfolded and damaged proteins and maintaining cellular homeostasis. Accumulation of misfolded and aggregated proteins is the hallmark of a number of neurodegenerative diseases, such as Parkinson's (Olanow and McNaught, 2006), Huntington's (Ortega et al., 2007) and Alzheimer's (Oddo, 2008). Enhancing proteasomal degradation is considered a promising strategy to ameliorate the phenotypes associated with diseases characterized by aberrant accumulation of proteinaceous aggregates (protein misfolding diseases). Our limited understanding of the regulatory mechanisms underlying activation of UPS function, however, precludes the rational design of pharmacological strategies to increase proteasomal degradation. As a result, proteasome activators are rare and remain poorly characterized.

1.1. The Ubiquitin Proteasome System

The UPS is one of the main intracellular proteolytic machineries that maintain protein homeostasis by mediating degradation of misfolded and damaged proteins. It is also involved in regulating the half-lives of proteins, thereby participating in key processes such as gene expression, cell cycle, and tumor development (Jariel-Encontre et al., 2008). Proteins targeted for degradation are labeled with ubiquitin (Ub) molecules, unfolded, and inserted into the proteasome for cleavage. The UPS is composed of the 26S proteasome, ubiquitin activating enzymes (E1), ubiquitin conjugating enzymes (E2), and ubiquitin ligases (E3) that mediate ubiquitination of substrate proteins (**Figure 1.1**). The 26S proteasome includes the 20S core particle (CP) and the 19S regulatory particles (RP). The ~700kDa barrel-shaped 20S CP is composed of 28 subunits (Rechsteiner and Hill, 2005 and Kish-Trier and Hill, 2013). Three active sites with trypsin-like, chymotryptsin-like, and caspase-like activities are embedded in the center of the barrel (Rechsteiner and Hill, 2005). Two ATP-independent activators (PA28 and PA200) and one ATP-dependent activator (the 19S RP, also known as PA700) regulate the 20S CP.

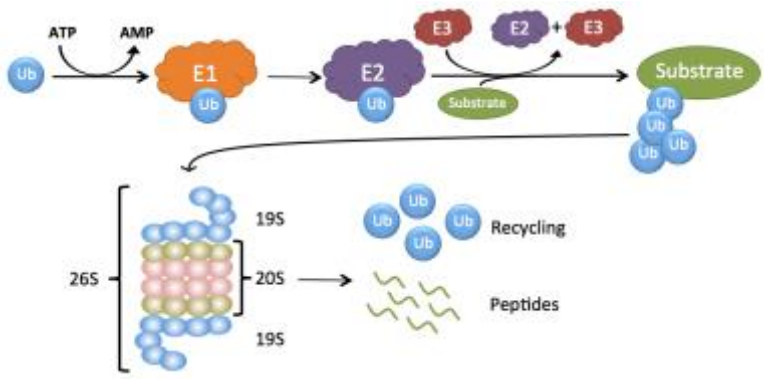

Figure 1.1. Overview of the UPS. Protein degradation is mediated by the UPS through sequential steps: i) activation of Ub mediated by the ubiquitin activating enzyme (E1); ii) Ub conjugation to the Ub-conjugating enzyme (E2); iii) Ub transfer from E2 to the substrate; iv) Ub chain elongation; v), degradation of polyUb-tagged substrates via the 26S proteasome.

Ubiquitination of proteins targeted for degradation proceeds through three steps (**Figure 1.1**): i) activation of ubiquitin catalyzed by an E1 enzyme; ii) conjugation of the activated ubiquitin to an E2 enzyme; iii) transfer of the activated ubiquitin from the E2 enzyme to the substrate catalyzed by an E3 ligase (Kleiger and Mayor, 2014, Scheffner et al., 1995 and Weissman et al., 2011). Depending on the ubiquitination patterns, the substrate may be internalized into the lysosome and degraded by the lysosomal hydrolytic enzymes or may be directed to the 26S proteasome for proteasome-mediated degradation (Kommander, 2009). In addition to the ubiquitin-dependent pathway, a ubiquitin-independent pathway also exists and mediates the degradation of aged, oxidized, or unfolded proteins (Jariel-Encontre et al., 2008).

1.2. Proteasome Modulators: Inhibitors and Activators

Proteasome inhibitors have been widely used in research (Huang and Chen, 2009) and have transitioned to clinical therapeutics (Burger and Seth, 2004). Both natural and synthetic inhibitors have been identified. Naturally occurring

proteasome inhibitors are classified as small molecule compounds such as tyropeptin A, PR39, lactacystin and epoxomicin (Huang and Chen, 2009), and macromolecular proteins, which are few and poorly characterized. Synthetic inhibitors include peptide aldehydes, reversible inhibitors such as leupeptin and MG-132, and irreversible inhibitors that form covalent bonds with the peptidase sites of the proteasome (Sander and Joung, 2014). Structural analyses helped decipher the mechanism of inhibition and enabled the rational design of both reversible and irreversible inhibitors with improved function (Bogyo and Wang, 2002).

A limited number of chemical activators of proteasomal degradation have been reported but remain poorly characterized. Denaturing reagents, lipids, and peptide-based molecules may activate the proteasome when present at high concentrations, but also induce significant toxicity (Huang and Chen, 2009). Oleuropein and betulinic acid were also reported to activate the proteasome (Huang and Chen, 2009). Oleuropein can activate all three hydrolytic sites, while betulinic acid activates the chymotrypsin-like active site without affecting the trypsin-like and caspase-like sites (Huang and Chen, 2009). Two other small molecules, AM-404 and MK-866, were recently discovered from the NIH NCC collection through a series of *in vitro* and *in cellulo* assays as proteasome agonists (Trader et al., 2017).

Three macromolecular protein complexes, PA28/11S REG, PA200/Blm10 and PA700/19S RP, are involved in the regulation of proteasome activity. Both PA28 and PA200 can bind to the 20S core and facilitate opening of the proteasome entrance

gate (Lee et al., 2010). The biological roles of PA28 and PA200 remain elusive. They are hypothesized to bind to each side of the proteasome barrel with synergistic effect (Rechsteiner and Hill, 2005). PA200 was reported to regulate the cellular localization of the 20S proteasome, but its physiological function remains unclear (Rechsteiner and Hill, 2005).

Overexpression of the 19S RP subunit PSMD11 was found to increase UPS activity and promote 26S assembly (Rechsteiner and Hill, 2005). The expression of PSMD11 is further regulated by the insulin/insulin-like growth factor-I FOXO4 in a cell-type dependent manner (Vilchez et al., 2012). Structural analyses demonstrate that PSMD11 contacts the C-termini of the 20S subunits and contributes to the overall stability of the 26S complex (Vilchez et al., 2012a). Overexpression of PSMD11 in *C. elegans* enhances protection against proteolytic stress and increases the longevity of the worm (Vilchez et al., 2012b). Disruption of PSMD11 causes death in *S. cerevisiae* (Kish-Trier and Hill, 2013). Further research demonstrated that phosphorylation of PSMD11 at the Serine 14 via the c-AMP pathway further enhances proteasome degradation (Lokireddy et al., 2015).

Deubiquitinating enzymes or deubiquitinases (DUBs) are also essential regulators of UPS function. They mediate removal of ubiquitin from substrates and participates in ubiquitin maturation, recycling, and editing (Huang and Chen, 2009 and Pfoh et al., 2015). They belong to the superfamily of proteases and can be further classified into five sub-classes based on the structure of their catalytic domains (Nijman et al., 2005). Among the five sub-classes, the ubiquitin-specific

proteases (USP) mediate ubiquitin-dependent protein degradation and display specificity for different substrates and E3 ligases. The yeast DUB Ubp6p and its mammalian homolog USP14 was shown to inhibit proteasome function via binding to the 19RP and to inhibit protein turnover, although the exact mechanism remains elusive (Hu et al., 2005 and Lee et al., 2010). The discovery that the deubiquitinating enzyme USP14 inhibits degradation of ubiquitinated substrates (Hanna et al., 2006) has led to the discovery of the proteasome activator IU1, a small-molecule inhibitor that selectively targets the activated form of USP14 (Lee et al., 2010). This study provides proof-of-principle demonstration of pharmacologic activation of proteasomal degradation.

Some ubiquitin ligases may also function as proteasome activators. The E3 ubiquitin ligase Parkin activates the 26S proteasome by promoting the interaction between the N-terminal ubiquitin-like domain and the 19S subunits (Saito et al., 1997). Mutations in *parkin* gene are associated with the early-onset autosomal-recessive familial Parkinson's disease, which is characterized by accumulation of misfolded and aggregated proteins (Um et al., 2010). Overexpressing C-terminus of the E3 ligase HSC70-interacting protein (CHIP) enhances degradation of Huntingtin, a protein that forms aggregates in association with the development of the Huntington's disease (Um et al., 2010). Overexpression of CHIP also promotes the degradation of p53 (Jana et al., 2005).

Despite increasing evidence describing the role of endogenous proteins in the regulation of proteasomal degradation, we are currently unable to rationally design

activators of UPS activity. This lack of knowledge motivates the development of high-throughput screens to identify UPS targets for activation of protein degradation.

1.3. The *e*Deg-On System: A Genetic Inverter for Monitoring Enhancement of UPS Activity

My lab has previously devised an orthogonal genetic circuit, the *e*Deg-On system (**Figure 1.2**), which links enhancement of UPS activity to an easily detectable fluorescent output (Zhao et al., 2014). Unlike other fluorescent protein reporters that link proteasomal degradation to a decrease in protein fluorescence (Dantuma et al., 2000, Li et al., 1998, and Hamer et al., 2010), the *e*Deg-On system is based on a positive correlation between *activation* of degradation and *increase* in GFP signal. The tetracycline repressor (TetR) was engineered to function as a UPS substrate by fusion to a degradation tag. Specifically, TetR was fused to the 16-residue CL1 hydrophobic peptide that mediates degradation of the fusion protein via the ubiquitin-dependent pathway (Gilon et al., 2000), or to the ODC, the 37-amino acid C-terminal sequence of ornithine decarboxylase that mediates degradation of the fusion protein via the ubiquitin-independent pathway (Dantuma et al., 2000). The circuit was then optimized using the tetracycline-controlled transactivator (tTA), a transcription factor that can function either as a repressor when bound to the tetracycline operator (TO) placed downstream of the promoter, or as an activator when bound to seven cassettes of TO placed upstream of a minimal CMV promoter

(Li et al., 1998). A tTA-based self-activation loop was included in the circuit to enhance the sensitivity and dynamic range of the output signal.

The CL1 degradation tag was discovered in the context of a yeast screen designed to isolate sequences that would destabilize the cytosolic yeast protein Ura3p, resulting in its degradation though the Ubc6p/Ubc7p system (Gilon et al., 1998). The CL1 tag was used to study ubiquitin-dependent degradation using fusion proteins such as Ura3p-CL1 in yeast and GFP-CL1 in mammalian cells and *C. elegans* (Metzger et al, 2008, Bence et al, 2001 and Link et al, 2006). The E3 ligase involved in the CL1 degradation pathway is Doa10 (yeast)/TEB4/March6 (human homolog) (Metzger et al., 2008), but the interacting DUB responsible for removing the ubquitin from the substrate in the CL1 degradation pathway has not been identified. A number of E3 ligases and DUBs mediating March6 degradation or CL1-independent March 6 substrate degradation have been identified, including WSB-1, USP19 and USP33 (Zavacki et al., 2009 and Nakamura et al, 2014).

The *e*Deg-On system (Zhao et al., 2014) is comprised of three plasmids: i) a plasmid expressing tTA fused to either the CL1 or the ODC degradation tag (tTA-Deg) under the control of a strong promoter (CMV) (ptTA); ii) a plasmid expressing tTA-Deg under a minimal promoter (Pmin) activated by tTA for output signal amplification (pTRE_tTA); and iii) a plasmid expressing GFP under the control of the tetracycline operator (TO) for fluorescence output (pTO_GFP). The *e*Deg-On system can be calibrated using tetracycline (Tc) to enable sensitive detection of a wide

range of UPS activation levels.

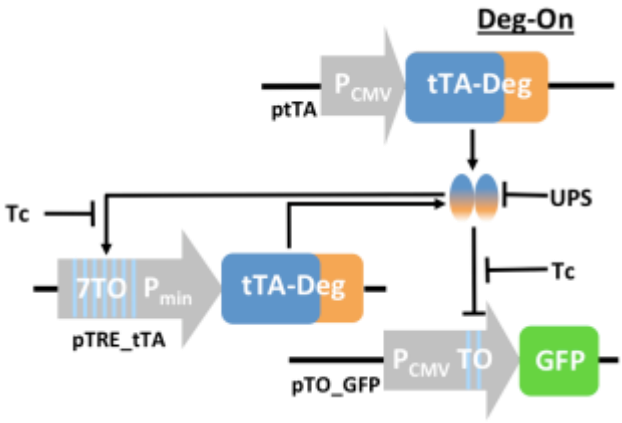

Figure 1.2. Diagram of the *e*Deg-On system.
The *e*Deg-On system contains three plasmids: ptTA for the expression of the tetracycline repressor variant (tTA) with a degradation tag (CL1 or ODC) under a strong promoter (CMV) with hygromycin resistance; pTRE_tTA for the expression of a self-activation loop of tTA under a minimal promoter (Pmin) for output signal maximization; and pTO_GFP for the expression of GFP under the control of the tetracycline operator (TO) for fluorescence output (Zhao et al., 2014).

1.4. CRISPR-cas System: Genome-editing Technology

The CRISPR-cas technology has emerged as a tool to introduce genetic modification in the chromosome. Discovered in bacteria, clustered, regularly interspaced, short palindromic repeat (CRISPR) sequences are processed by CRISPR-associated protein nucleases (cas) to target invading foreign DNA, such as viruses and plasmids (Sampson and Weiss, 2014). The CRISPR system has been adopted for genome engineering purposes and it is typically based on the use of the *Streptococcus pyogenes* single cas9 nuclease (Sander and Joung, 2014).

In addition to the cas9 nuclease, the CRISPR-cas system also requires a guide RNA (gRNA) comprised of two RNA segments: a sequence complementary to the genomic sequence to be cleaved (CRISPR RNA or crRNA), and a transactivating CRISPR RNA (tracrRNA) to mediate formation of a complex between the genomic DNA and cas9 (Sander and Joung, 2014). As a complex, the cas9 protein and the

engineered gRNA can target and cleave double-stranded DNA in any genomic region, including coding sequences, promoters, and regulatory elements. Two different DNA repair pathways are responsible for repairing the double strand break introduced by the cas9/gRNA complex, and introduce different mutations into the genome. Random insertions/deletion (indel) mutations are introduced via the nonhomologous end joining (NHEJ) DNA repair pathway, resulting in premature stop codon or out of frame mutations that knock out the gene (Sander and Joung, 2014). Alternatively, a sequence of interest can be inserted in the genome through the homology-directed repair (HDR) pathway at a site targeted by the gRNA (Sander and Joung, 2014). The sites targeted with gRNA can either locate in the middle of an exon to allow the precise insertion of an exon sequence with a specific mutation (Gratz et al., 2014 and Lin et al., 2014) or downstream of a gene of interest to fuse the gene of interest to a tag or to a reporter gene (Gratz et al., 2014 and Yang et al., 2013).

CRISPR also has applications beyond genome editing. Cas9 harboring the D10A and H840A substitutions lacks endonuclease activity: this “dead” cas9 (dcas9) can be used as a genome interference tool for transcriptional repression and activation (Qi et al., 2013, Cong et al., 2013, Mali et al., 2013 and Larson et al., 2013). Dcas9 does not introduce double strand breaks into the genomic sequence due to the lack of endonuclease activity, but binds to the genomic region complementary to gRNA and helps recruit repressors or activators when bound to the promoter region. For transcriptional activation, dcas9 can be coupled with engineered transcription activation domains, such as antibody epitope-fused VP64 chains or a combination of

VP64, HSF1, and p65 activation domains (Heckl and Charpentier, 2015). To achieve transcription repression, dcas9 is usually fused to repressive chromatin-modifying complexes such as the Krüppel-associated box(KRAB) domain (Gilbert et al., 2013).

The CRISPR technology has been used not only to introduce individual gene modifications in a variety of prokaryotic and eukaryotic organisms including microorganisms, animals, plants (Sanger and Joung, 2014), and even human embryos (Liang et al., 2015), but also to achieve whole-genome scale modifications in human and mouse cell lines (Shalem et al., 2014, Wang et al., 2014, Hart et al., 2015, Ma et al., 2015, Doench et al., 2016 and Tzelepis et al., 2016). CRIPSR-cas lentiviral libraries containing gRNAs for all nonessential genes have been introduced to mammalian cell lines, and subpopulations presenting desired properties, such as drug resistance, were isolated and subjected to next-generation sequencing (Wang et al., 2014 and Shalem et al., 2014 and Sanjana et al., 2014).

1.5. GeCKO Library and Applications

A number of CRISPR-based libraries were developed to introduce indel mutations throughout the entire genome and to achieve whole-genome knockout. Among these pooled libraries, the second generation of the human genome-scale CRISPR-Cas9 knockout (GeCKOv2) library is of special interest because it provides broad coverage of the human genome and miRNAs (Sanjana et al., 2014). This lentivirus-based library is divided into two sub-libraries with each sub-library containing three gRNAs per gene that can be used for smaller-scale knockout

screens. This GeCKOv2 library can be introduced into the HEK293/*e*Deg-On cells for the identification of proteasome modulators that enhance proteasome activity upon knockout.

The GeCKOv2 library has been utilized in a variety of screening strategies (Shalem et al., 2015). It is mostly used for genome-wide drug resistance screens, where a primary cell line is transduced with GeCKOv2 library and treated with the drug of interest to select genes involved in the cell response to drug treatment. The GeCKOv2 library can also be introduced into a stable cell line in which the expression of a fluorescence reporter is linked to a gene of interest to identify genes that affect the expression of the gene of interest via fluorescence-activated cell sorting (FACS).

Chapter 2

Results

2.1. Establishing HEK293/*e*Deg-On_2 Stable Cell Lines

The current *e*Deg-On system is based on the use of puromycin as antibiotic selection marker and it cannot be used to screen the GeCKOv2 library, which is also based on puromycin selection. To overcome this limitation, the puromycin cassette in the plasmid expressing tTA (ptTA) was replaced with a hygromycin cassette, generating the plasmid ptTA_2. Standard restriction enzyme cloning was used to replace the puromycin resistance gene with the hygromycin resistance gene (**Figure 2.1**), and the sequence was verified by Sanger sequencing.

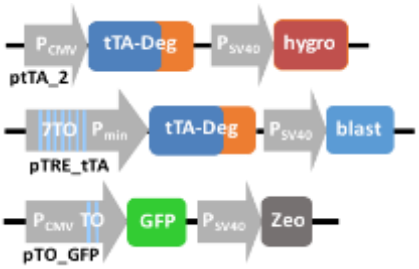

Figure 2.1. The *e*Deg-On_2 system. The *e*Deg-On_2 system is composed of three plasmids: i) ptTA_2 containing the hygromycin selection marker; ii) pTRE_tTA containing the blasticidin marker; and iii) pTO_GFP containing the zeocin marker.

To establish a new cell line with chromosomal integration of the *e*Deg-On_2 system, a cell line stably transfected for the expression of the TO_GFP cassette was developed first. HEK293 cells were transfected with pTO_GFP, cultured in the presence of zeocin for three weeks, and sorted to select the top 20% of cells presenting highest GFP expression. The resulting cells (HEK293/TO_GFP_2 cells) were co-transfected with ptTA_2 and pTRE_tTA, cultured in the presence of hygromycin and blasticidin, and sorted to select the 20% of cells presenting the lowest GFP expression. Sorted cells (HEK293/*e*Deg-On_2) were plated at 0.5 cell/well in 96-well plates to isolate monoclonal populations. Single clones (**Figure 2.2a**) were first treated without Tc and with 1 µg/ml Tc to monitor changes in GFP fluorescence in response to changes in Tc via flow cytometry (**Figure 2.2b**). It is expected that cells will not display fluorescence when tTA is bound to the TO operator upstream of GFP, and that when tTA is not bound to the TO operator, cells will display high fluorescence. The fluorescence signal is expected to increase as a function of the extent of tTA displacement from the operator to a maximum equal to the GFP fluorescence of the HEK293/TO_GFP_2 cells. However, GFP expression was found to be leaky, as signal was detected in the absence of Tc, suggesting basal expression of GFP in the presence of tTA. GFP expression at high Tc concentration is

also found to be lower than that of the parental HEK293/TO_GFP_2 cells, suggesting residual binding of Tc-bound tTA to the operator, as expected (Zhao et al., 2014). Single clones presenting increase in GFP fluorescence upon addition of Tc equal or higher than half of the theoretical expected increase were selected for further analyses.

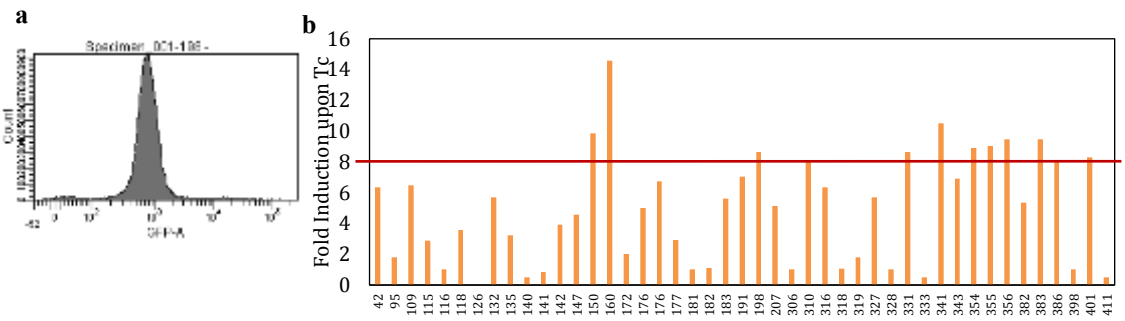

Figure 2.2. Fluorescence of isolated HEK293/*e*Deg-On_2 single clones.
a, Example of a single clone with a single peak in fluorescence without Tc; x-axis, GFP fluorescence; y-axis, cell number. **b**, GFP fluorescence intensity of single clones reported as ratio of cell fluorescence in the presence of Tc to cell fluorescence of untreated cells; clones presenting increase in GFP fluorescence upon addition of Tc equal or higher than half of the theoretical expected increase (red line) were selected for further analyses; y-axis, fold change in fluorescence.

The fluorescence of selected HEK293/*e*Deg-On_2 single clones was also evaluated in response to treatment with the proteasome inhibitor MG132 (**Figure 2.3**). All clones were tested without Tc or with 0.2 µg/ml Tc and with 3 µM of MG132. With the exception of clone 355, all cells treated with MG132 showed a 1.6-fold or higher decrease in fluorescence when treated with 0.2 µg/ml Tc, suggesting that these clones are sensitive to decrease in proteasome activity.

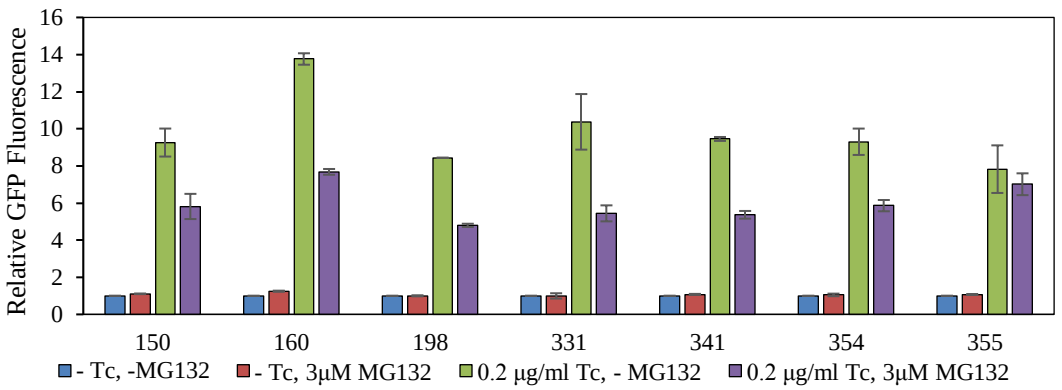

Figure 2.3.GFP fluorescence of HEK293/*e*Deg-On_2 single clones in response to treatment with the proteasome inhibitor MG132.
Relative GFP fluorescence values were calculated by normalizing the fluorescence of treated cells to that of control cells cultured without Tc or MG132.

The HEK293/*e*Deg-On_2 clone #198 was selected as a candidate to test the proteasome activator PSMD11. PSMD11 was found to upregulate proteasome activity via phosphorylation, and the phosphomimetic PSMD11-S14D mutant can further enhance proteasome activation (Lokireddy et al., 2015). Cells transfected with a plasmid expressing PSMD11 displayed a 30% increase in GFP fluorescence, and cells transfected with a plasmid expressing PSMD11-S14D mutant showed a 38% significant increase in GFP fluorescence (**Figure 2.4**) compared to cells transfected with the control plasmid (pcDNA3.1+). This result suggests that the *e*Deg-On_2 system can detect proteasome activation induced upon overexpression of PSMD11 and PSMD11-S14D.

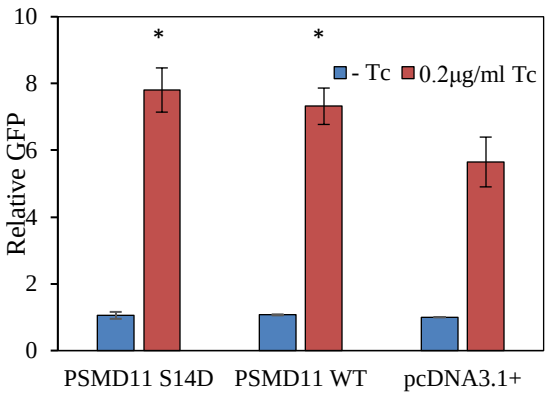

Figure 2.4. GFP fluorescence output of HEK293/*e*Deg-On_2 clone #198 upon overexpression of PSMD11 and PSMD11-S14D.
GFP fluorescence of cells transfected with PSMD11-S14D, PSMD11 and pcDNA3.1+ (control) plasmids were measured without and with 0.2 µg/ml Tc. Relative GFP fluorescence values were calculated by normalizing the fluorescence of cells transfected with PSMD11 or PSMD11-S14D plasmids to that of cells transfected with the control plasmid without Tc.

2.2. Verifying CRISPR-mediated Knockout Controls

Positive controls for the knockout screen based on introducing the CRISPR-mediated library to HEK293/*e*Deg-On_2 cells were established. A lentiviral plasmid (pLentiCRISPRv2) was generated to target a single gene (**Figure 2.5**). It contains the 20bp gRNA complementary to the knockout region and the *cas9* sequence for DNA cleavage. It also contains a puromycin selection marker for selection purposes. Two different gRNAs were designed and inserted into the lentiCRISPRv2 vector: a) the gRNA targeting tTA, and b) a control nontargeting (NT) gRNA, a 20bp gRNA sequence that does not target any known coding sequence in the human genome.

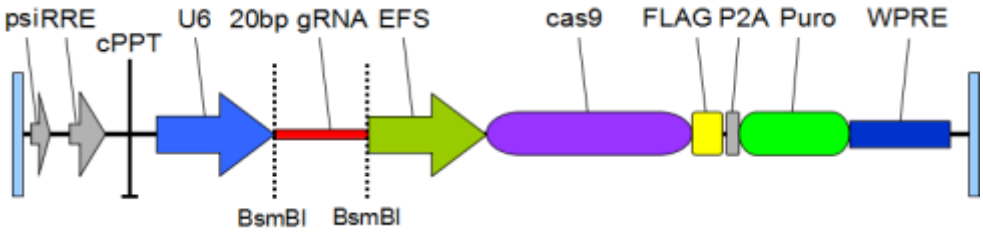

Figure 2.5. pLentiCRISPRv2 with gRNA of interest.
plentiCRISPRv2 contains the 20bp gRNA complementary to a specific sequence in the gene targeted for knockout, the cas9 gene for DNA cleavage, and the puromycin resistance cassette.

The effect of tTA knockout on GFP fluorescence was evaluated in HEK293/*e*Deg-On_2 cells. The GFP fluorescence of cells transduced with viruses expressing tTA-specific gRNA was found unchanged upon Tc dosage, while the GFP fluorescence of cells transduced with viruses expressing non-targeting gRNA increased as a function of Tc concentrations (**Figure 2.6**). This result suggests that CRISPR-mediated tTA knockout alters the GFP expression of the *e*Deg-On_2 system.

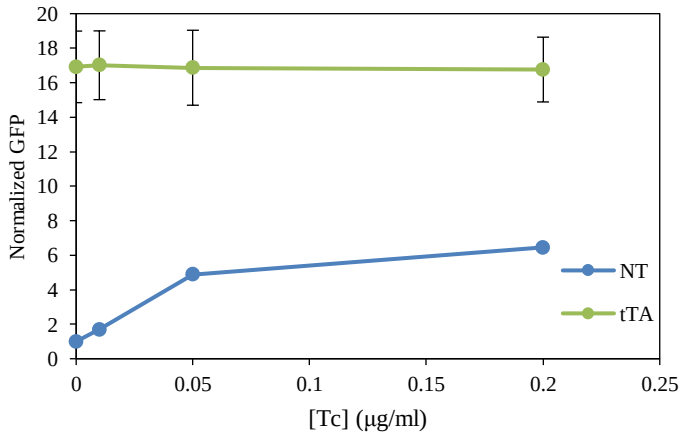

Figure 2.6. Transduction of HEK293/*e*Deg-On_2 clone #198 with NT and tTA gRNA viruses. HEK293/*e*Deg-On_2 cells were transduced with equal number of virus particles of NT or tTA gRNA viruses and selected using puromycin at 1 µg/ml for one week. Cells were replated and treated with different Tc concentrations for 24 hours before analysis on flow cytometry. All GFP fluorescence was normalized to that of NT-gRNA virus transduced cells without Tc.

2.3. Titration of CRISPR-mediated Knockout Viruses

Virus titration was conducted to determine the amount of virus needed to transduce cells such that >90% of transduced cells receives only one copy of virus per cell. Three titration methods are most commonly used: a) RNA titration to assess the copy number of viral genome in the viral supernatant; b) DNA titration to quantify viral integration into the mammalian host genome; c) functional titration to evaluate the expression of the transgene (a fluorescence reporter gene or a gene conferring antibiotic resistance) encoded in the viral genome (Sastry et al., 2002).

The RNA titration method was used in this study to estimate the titers of tTA and NT gRNA viruses. The titers (number of virus particles per volume) of different gRNA viruses were found to be in the same order of magnitude (**Figure 2.7**). The RNA titration method was reported to overestimate the real titer, because the RNA titer also takes defective viral particles into account (Scherr et al., 2001, Sastry et al, 2002 and Geraerts et al., 2006).

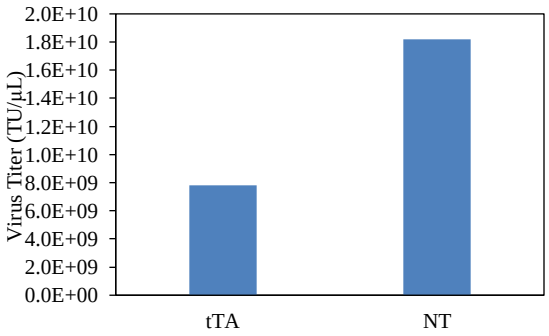

Figure 2.7. Titers for tTA and NT gRNA viruses.
Y axis, virus titer (transducing unit per microliter of concentrated virus).

Compared to the RNA titration method, the functional titration method, which is typically based on a measurement of fluorescence or cell survival, was reported to provide a more accurate estimate of the number of viable viral particles (Sastry et al., 2002). Because the GeCKOv2 lentiviral plasmids contain gene conferring antibiotic resistance, the functional titer in this study was determined by monitoring cell viability after antibiotic selection of transduced cells. Poisson statistics helps to establish links between cell viability and the multiplicity of infection (MOI), which is defined as the ratio of viral particles to transduced cells (Shabram and Aguilar-Cordova, 2000). Based on Poisson distribution, conducting

transduction at an MOI of 0.2 allows approximately 90% of the cells surviving antibiotic selection to be transduced with only one copy of virus (Sanjana et al., 2014). The amount of concentrated virus equivalent to an MOI of 0.2 for a total of $8*10^4$ transduced cells with either NT and tTA gRNA virus was determined to be 6 μL, and this amount was scaled up for mock screen studies.

2.4. Mock Screen in HEK293/*e*Deg-On_2 Cells

2.4.1. Experiment 1: Transduction of HEK293/*e*Deg-On_2 cells with different ratios of NT and tTA gRNA viruses

To evaluate whether the *e*Deg-On_2 system can be used to distinguish the fraction of cells in which tTA is knocked out by monitoring changes in the cell fluorescence output, HEK293/*e*Deg-On_2 cells were transduced with NT gRNA virus, tTA gRNA virus, or different ratios of a NT/tTA gRNA virus mixture. Cells transduced with tTA gRNA viruses showed an 18-fold increase in GFP fluorescence compared to cells transduced only with NT gRNA virus (**Figure 2.8**). Cells transduced only with NT gRNA viruses were used as negative control, and the 1% gate was established by the top 1% cells with highest fluorescence in the negative control cells. The number of cells above the 1% gate was monitored and the numbers of expected hits and actual hits in cells above the gate were calculated (**Table** 2.1). The expected hits were defined as positive control cells (cells transduced only with tTA gRNA virus) that was expected to be in the gated population and the number of expected hits was calculated by multiplying the

number of cells above the 1% gate in cells transduced only with tTA gRNA viruses by the tTA gRNA: NT gRNA virus transduction ratio. The actual hits were defined as cells experimentally measured in the gated population that were not false positives and was calculated by subtracting the number of cells above 1% gate among the population of cells transduced only with NT gRNA virus (false positives) from the number of cells above 1% gate among cells transduced with the virus mixture. For the ratios of NT gRNA: tTA gRNA of 1000:1 and 100:1, the *e*Deg-On_2 system was found to detect changes in the number of cells above the 1% gate, and the numbers of expected hits and actual hits were similar. However, the *e*Deg-On_2 system could not be used to distinguish cells transduced with tTA gRNA viruses from cells transduced with NT gRNA viruses at 10000:1 ratio.

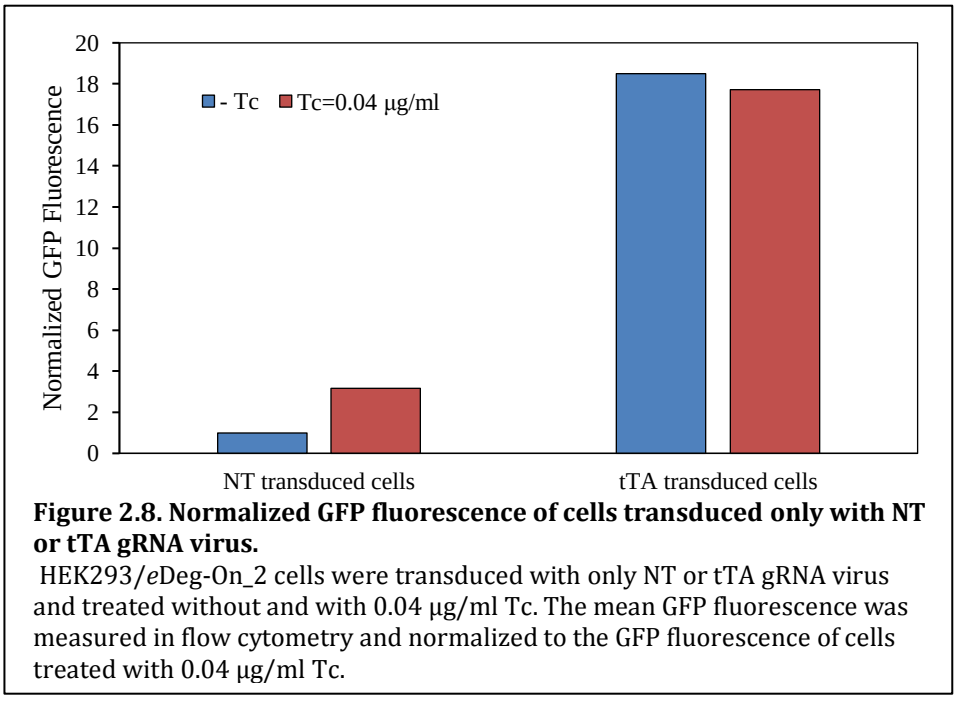

Figure 2.8. Normalized GFP fluorescence of cells transduced only with NT or tTA gRNA virus.
HEK293/*e*Deg-On_2 cells were transduced with only NT or tTA gRNA virus and treated without and with 0.04 µg/ml Tc. The mean GFP fluorescence was measured in flow cytometry and normalized to the GFP fluorescence of cells treated with 0.04 µg/ml Tc.

Table 2.1.Mock screen experiment 1 results.

- Tc				Tc=0.04 μg/ml			
Sample	# Cells above 1% gate	# Expected hits	# Actual hits	Sample	# Cells above 1% gate	# Expected hits	# Actual hits
NT only	1041	-	-	NT only	1017	-	-
100:1	2836	1361	1795	100:1	3103	251	2086
1000:1	1207	1073	166	1000:1	1130	25	113
tTA only	31998	-	-	tTA only	25129	-	-

To detect weaker proteasome activators, the *e*Deg-On_2 system may be fine-tuned with Tc to adjust detection sensitivity. To evaluate the effect of Tc on the output signal, transduced cells were treated with 0.04 μg/ml Tc. Cells transduced with tTA gRNA virus and treated with 0.04 μg/ml Tc display a 5.6-fold increase in GFP fluorescence compared to cells transduced only with NT gRNA virus (**Figure 2.8**). Similar results were obtained for cells transduced using 100:1 and 1000:1 ratios of NT gRNA: tTA gRNA viruses in the presence of 0.04 μg/ml Tc (**Table** 2.1), suggesting that the *e*Deg-On_2 system may be used to distinguish cells transduced with tTA gRNA virus from cells transduced with NT gRNA virus in the presence of 0.04 μg/ml of Tc. In conclusion, the *e*Deg-On_2 system can detect a minimum ratio of 1000 to 1 between cells transduced with NT- and tTA-gRNA virus either without Tc treatment or with 0.04 μg/ml Tc.

2.4.2. Experiment 2: Evaluation of the signal of the *e*Deg-On_2 system using different ratios of cells treated with different amounts of Tc

The previous experiment provided information on the signal of the *e*Deg-On_2 system when strong proteasome activators similar to that of tTA knockouts

are available. Weaker knockout controls than the tTA knockout are needed so that the *e*Deg-On_2 system can be evaluated under different levels of proteasome activation. However, we lack such a positive control. Instead of testing proteasome activators upon knockout, it is possible to directly test whether cells with increased fluorescence can be distinguished from a larger population of cells with basal fluorescence.

To evaluate whether the *e*Deg-On_2 system can distinguish a small fraction of cells with increased fluorescence from a population of cells with basal fluorescence, HEK293/*e*Deg-On_2 cells were treated with different concentrations of Tc, and the GFP fluorescence was measured using flow cytometry (**Figure 2.9**). Cells treated with 0.04 μg/ml Tc were used as negative control and were mixed with cells treated with a higher Tc concentration (0.1 or 1 μg/ml) at different ratios (100:1 and 1000:1). A 1% gate was established by the top 1% cells displaying highest fluorescence among the population of negative control cells. The number of cells above the gate, the number of expected hits and the number of actual hits were quantified (**Table** 2.2). For both mixtures of cells treated with ratios of low (0.04 μg/ml) to high (0.1 or 1μg/ml) Tc concentration of 100:1 and 1000:1, the *e*Deg-On_2 system enables reliable detection of changes in the number of cells above the 1% gate, and the number of actual hits is in agreement with the number of expected hits.

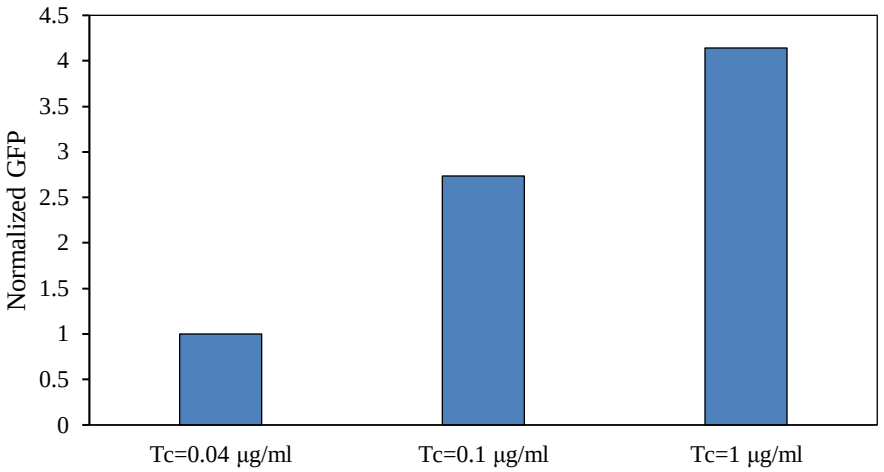

Figure 2.9. Normalized GFP fluorescence of cells treated with different concentration of Tc.
HEK293/*e*Deg-On_2 cells were treated with different concentrations of Tc (0.04, 0.1 and 1 µg/ml). The mean GFP fluorescence was measured using flow cytometry and normalized to the GFP fluorescence of cells treated with the 0.04 µg/ml Tc.

Table 2.2. Mock screen experiment 2 results.

1% gate				2% gate			
1000:1				1000:1			
Sample	# Cells above 1% gate	# Expected hits	# Actual hits	Sample	# Cells above 2% gate	# Expected hits	# Actual hits
0.04 only	1031	-	-	0.04 only	2079	-	-
0.04+ 0.1	1044	4	13	0.04+ 0.1	2152	15	73
0.04+1	1068	19	37	0.04+1	2121	50	42
100:1				100:1			
Sample	# Cells above 1% gate	# Expected hits	# Actual hits	Sample	# Cells above 2% gate	# Expected hits	# Actual hits
0.04 only	1003	-	-	0.04 only	2026	-	-
0.04+ 0.1	1011	44	8	0.04+ 0.1	2112	146	86
0.04+1	1204	190	201	0.04+1	2548	505	522

To evaluate whether establishing a larger gate would help enrich the representation of actual hits in the total gated cells, a 2% gate was also set based on the top 2% of cells displaying the highest fluorescence among the population of cells

treated only with 0.04 μg/ml Tc. The number of cells above the 2% gate, the number of expected hits and the number of actual hits were quantified (**Table** 2.2). To compare the 2% gate and the 1% gate, the percentage of actual hits in the total population were calculated for the cell mixtures at 100:1 ratio (**Table** 2.3). The percentage increase from 1% to 2% gate, suggesting that increase in gating from 1% to 2% enriches the representation of hits in the gated population.

Table 2.3. Comparison of gating in experiment 2.

Sample	# Actual hits above 1% gate	# Actual hits above 2% gate	% Actual hits above 1% gate in the total population	% Actual hits above 2% gate in the total population
0.04+0.1	8	86	0.008%	0.086%
0.04+1	201	522	0.201%	0.522%

2.4.3. Summary for Experiment 1 and 2

The goal of the mock screens (experiment 1 and 2) was to evaluate the *e*Deg-On_2 system as a reporter assay for the GeCKOv2 library screen. The robustness of a reporter assay is critical for conducting a pooled library-based screen and it is evaluated by quantifying the dynamic range and the signal-to-noise ratio (Hu and Luo, 2012). Experiment 1 was used to evaluate the dynamic range of the *e*Deg-On_2 system by comparing the GFP fluorescence of cells transduced only with NT gRNA virus to the fluorescence of cells transduced only with tTA gRNA virus, and a 5.6-fold increase in GFP fluorescence was observed with 0.04 μg/ml Tc. Another fluorescence-based assay reported a similar fold increase (6 fold) in fluorescence between negative and positive control in a GeCKO library screen (Timms et al., 2016), suggesting that the dynamic range of the *e*Deg-On_2 system was suitable for

a GeCKO library screen. Another method was utilized to evaluate the dynamic range of the reporter assay. This method establishes a 1% or 2% gate by gating top 1% or 2% cells with highest fluorescence in the negative control, and compares the percentage of cells in this gate in the positive control to the established 1% or 2% cells in the negative control. In the NT/tTA gRNA virus transduction experiment, with the 1% gate determined by the top 1% cells with highest fluorescence in NT gRNA virus transduced cells, the percentage of cells above the 1% gate for tTA gRNA transduced cells was found to 25.1% (25,129 cells in the 1% gate out of a total of 100,000 cells) at 0.04 μg/ml Tc. Similarly, another reporter assay used in another GeCKO library screen reported an increase from 1% to 26.8% in transduced cells (Wu et al., 2016). Therefore the dynamic range of the *e*Deg-On_2 system satisfies the requirement of a CRISPR-based knockout screen.

To evaluate the signal-to-noise ratio of the *e*Deg-On_2 system, different ratios of positive and negative controls were mixed and cell numbers in the top 1% gate were monitored using flow cytometry. Two different sets of positive and negative controls were used in the mock screens. The first set utilizes cells transduced only with tTA gRNA viruses as positive control and cells transduced only with NT gRNA viruses as negative control. Different ratios of NT and tTA gRNA viruses were then used to transduce cells to mock the different representations of strong proteasome activators in the library. These strong proteasome activators upon knockout are expected to have GFP fluorescence similar to the fluorescence of tTA knockouts. The result of the NT/tTA gRNA virus transduction experiment suggests that the *e*Deg-On_2 system can detect a minimum of 120 gRNA hits among a library of about

120,000 gRNAs. If the library contains fewer than 120 hits, the noise of the *e*Deg-On_2 system may result in a high rate of false negatives.

The second set of positive and negative controls utilizes cells with higher fluorescence treated by a higher Tc concentration as positive control and cells with lower fluorescence treated by lower Tc concentration as negative control. Different ratios of cells treated with higher Tc concentration were mixed with cells treated with lower Tc concentration to mock the different representations of proteasome activators in the library. The result of the high/low Tc treatment experiment suggests that the *e*Deg-On_2 system is capable of detecting about 120 hits among a library of about 120,000 gRNAs if on average these 120 hits can introduce increased fluorescence beyond 2.5 fold. The signal-to-noise ratio is poor if fewer than 120 hits with increased fluorescence of 2.5 fold or 120 hits with increased fluorescence below 2.5 fold are present in the library.

There are multiple possible methods to enhance the signal-to-noise ratio. Increasing library coverage is an effective approach to overcome poor signal resolution and to identify weaker hits present in pooled shRNA library screens (Strezoska et al., 2012). Increasing library coverage is also expected to facilitate the identification of hits characterized by low output signal or low representation in the context of a CRISPR-based library screen. Extending gating from 1% to 2% also enriches the representation of hits in the total population. Performing additional rounds of sorting is also expected to enrich the hits in the total population.

In summary, the results of the mock screens suggest that the *e*Deg-On_2 system provides a robust reporter assay for the screen of proteasome activators upon knockout via transduction of the GeCKOv2 library.

2.5. Screening with the GeCKOv2 Library

2.5.1. Considerations for MOI and Gating

HEK293/*e*Deg-On_2 cells will be transduced with the GeCKOv2 library and screened for selection of cells presenting increased fluorescence to isolate regulatory proteins that result in activation of proteasomal degradation upon knockout. The MOI and gating will be adjusted during sorting to tune the number of hits. The MOI determines the number of gRNAs in each cell. The gate will be determined by defining the cell population displaying highest fluorescence among a population of negative control cells that are transduced only with NT gRNA virus, as reported previously (Timms et al., 2016). The gating for sorting can also be determined by using the population of transduced cells with highest fluorescence (Wu et al., 2016 and DeJesus et al., 2016). Establishing the gate based on negative control cells will be more informative than directly establishing the gate with transduced cells, because the change in fluorescence of the hits can be compared directly to negative control cells.

2.5.2. Experimental Design

A preliminary screen will be first conducted using HEK293/*e*Deg-On_2 cells transduced with the GeCKOv2 library at 10X library coverage (**Figure 2.10**), and the MOI and the gate to be used will be determined based on the percentage of actual hits of the gated population. An MOI of 0.2 and a 1% gate would be first tested to determine if the percentage of actual hits is between 0.01% (equivalent to 12 gRNA hits in a total library of 120,000 gRNAs) and 1% (equivalent to 1200 gRNA hits in a total library of 120,000 gRNAs). Three outcomes are possible:

a) If the percentage of actual hits is above 1% of the total cell population, the gate will be lowered. If the percentage of actual hits still exceeds 1% with the 0% gate, the final screen will be conducted with 500X library coverage, and the top 1% cells with highest fluorescence will be gated among cells transduced with the GeCKOv2 library.

b) If the percentage of actual hits is between 0.01% and 1%, the final screen will be conducted with 500X library coverage at an MOI of 0.2.

c) If the percentage of actual hits is below 0.01%, the gate will be increased to 2%. If the percentage of actual hits is still below 0.01% with 2% gate, an MOI of 0.2 is not suitable for the screen with the GeCKOv2 library.

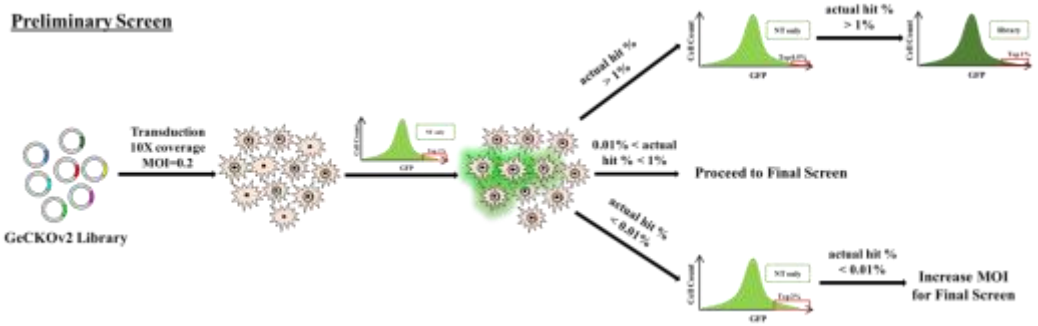

Figure 2.10. Preliminary screen plan.
The preliminary screen will be conducted with a smaller coverage compared with the final screen, and will determine the MOI and gating to be used in the final screen.

If performing transduction with an MOI of 0.2 does not result in an increase in the percentage of actual hits to 1%, the evaluation process will be repeated increasing the MOI to 1 (60% of cells is transduced with one or more gRNAs at MOI of 1). If a transduction with an MOI of 1 does not result in an increase in the percentage of cells above the 1% gate, an MOI of 5 will be tested, which corresponds to more than 99% of cells transduced with one or more gRNAs. If a transduction with an MOI of 5 still does not result in an increase the percentage of cells above the 1% gate, the current *e*Deg-On_2 system is not suitable for conducting the screen of proteasome activators upon knockout via transduction of the GeCKOv2 library.

The MOI and percentage of gating determined in the preliminary screen will be used to conduct the final screen at 500X coverage of the library (**Figure 2.11**). The gated population will be sorted, and hits will be enriched with additional rounds of sorting until the final population above the gate is more than 90% of the total cell population. Depending on the MOI used, different methods will be employed to obtain the gRNA representations as detailed below.

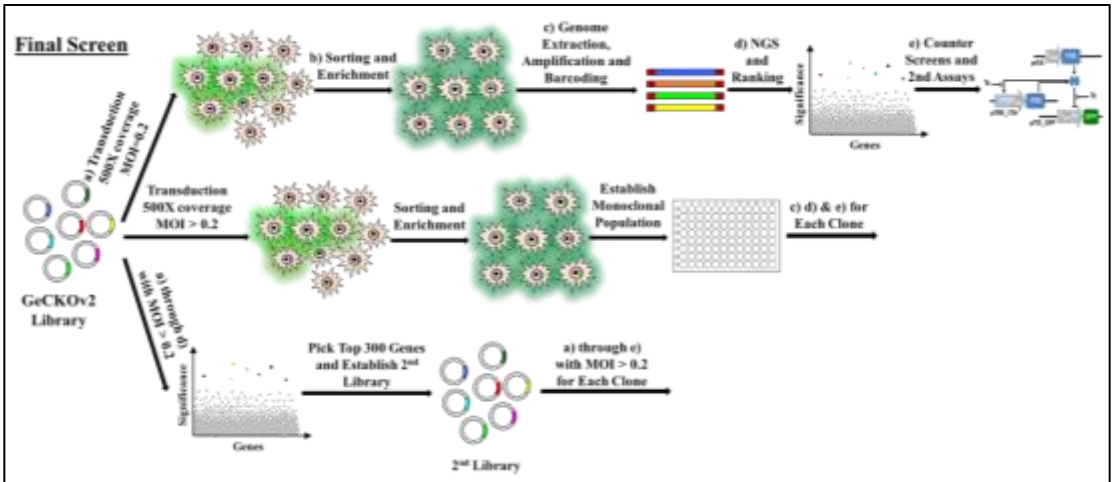

Figure 2.11. Final screen plan.
The final screen will be conducted at 500X coverage. Depending on the MOI determined in the preliminary screen, different methods to obtain and evaluate hits will be utilized.

If an MOI of 0.2 is used, the DNA of the final sorted population will be extracted, followed by the amplification of the gRNA regions and the addition of barcodes through PCR for next-generation sequencing. Next-generation sequencing will be used to determine the gRNA representations, and the gRNA representation of sorted cells will be compared to the gRNA representation of unsorted cells. Genes will be ranked based on enrichment of gRNA representations upon sorting via one or more of the algorithms including RSA (König *et al.*, 2007), RIGER (Luo *et al.*, 2008), HiTSelect (Diaz *et al.*, 2015) and MAGeCK (Li *et al.*, 2014). After gene ranking, the top ranked genes will be selected for validation as proteasome activators through counter screens, secondary assays, and other functional assays that detect UPS activation or study the specific function of these genes related to UPS.

If an MOI larger than 0.2 is used, two options are available. The first option to identify potential proteasome regulators is to directly establish monoclonal populations from sorted cells and use next-generation sequencing to determine the

proteasome activator(s) in each clone. Detailed steps of this option include: i) establish monoclonal populations from sorted cells; ii) extract genomic DNA from the monoclonal populations; iii) use next-generation sequencing to determine and compare gRNA representations of each monoclonal population to the unsorted population. One or few genes is expected to be highly enriched when comparing the unsorted population to the sorted population, and the gene or the combination of genes will be validated as proteasome activator(s) through counter screens, secondary assays, and other functional assays.

The second option to identify potential proteasome regulators is to establish a secondary library from the top hits of the primary screen and conduct a secondary screen using the secondary library. In addition to the primary screen, sometimes a secondary screen is used to validate the result of the primary screen. A secondary library was developed based on the top-ranked 300 genes in a GeCKOv2 library primary screen, and hits discovered from the secondary screen strongly supported the result of the primary screen (DeJesus *et al.*, 2016). Detailed steps of the second option include: i) perform steps from genome extraction to next-generation sequencing analysis as in the experiment conducted with an MOI of 0.2 and pick top 300 genes to establish a secondary library via oligo synthesis and re-cloning of the most potent gRNA targeting each of these 300 genes. If oligo synthesis is not an option, obtain amplified gRNA regions from the primary screen without establishing monoclonal populations and re-clone into lentiviral plasmids to obtain a secondary library; ii) produce virus from the secondary library, transduce HEK293/*e*Deg-On_2 cells with the same MOI and use the same gating for sorting; steps iii) and iv) are the

same as in the first option. The second option also shares the same expected outcomes and the validation of the hits through counter screens and secondary assays.

Chapter 3

Summary and Future Work

This project aims at optimizing the *e*Deg-On system and evaluating it for the discovery of proteasome activators through CRISPR-mediated whole-genome knockout screens. This goal was achieved by generating a stable cell line expressing the *e*Deg-On circuit that is compatible with CRISPR-cas system, and by evaluating this cell line for high-throughput screens. The stable cell line resulting from chromosomal integration of the *e*Deg-On circuit into HEK293 cells was validated by testing the GFP output signal in response to the inducer tetracycline, the proteasome inhibitor MG132, and the proteasome activators PSMD11 and PSMD11-S14D. A mock screen was also conducted by testing the response of the stable cell line to transduction with virus particles expressing gRNA specific for the gene encoding tTA and non-targeting gRNA to evaluate the use of this system in the contest of a high throughput screen.

3.1. Developing of the Stable Cell Line of the *e*Deg-On System

The *e*Deg-On_2 system is comprised of three components in three plasmids. The TO_GFP plasmid encodes the GFP gene downstream of the TO that results in regulation of GFP expression upon binding of tTA. A stable cell line with the TO_GFP component (pTO_GFP) was first generated via transfection, antibiotic selection for stable integration, and sorting for GFP-expressing cells with highest fluorescence. The two tTA plasmids (ptTA_2 and pTRE_tTA) were transfected into the newly developed HEK293/TO_GFP_2 cell line, followed by antibiotic selection for stable integration, and isolation of single clones with low GFP fluorescence.

Isolated HEK293/*e*Deg-On single clones were first tested in the presence of Tc, and single clones presenting increase in GFP fluorescence upon addition of Tc equal or higher than half of the theoretical expected increase were selected for further analyses. Selected clones were then evaluated in the presence of Tc for proteasome inhibition and activation. Most clones demonstrated a 1.6-fold or higher decrease in GFP fluorescence in response to the proteasome inhibitor MG132. Clone 198 was selected as a candidate to test its response to the proteasome activator PSMD11 and PSMD11-S14D, and approximately 1.3- and 1.4-fold increase in GFP were observed, respectively.

In summary, the following procedures for establishing and selecting a candidate clone for the *e*Deg-On system are recommended: 1) establish a monoclonal population of HEK293 cells stably transfected for the expression of the pTO_GFP plasmid that presents the highest GFP expression; 2) transfect the two tTA

plasmids (ptTA_2 and pTRE_tTA) into the newly developed cell line cell line at a ratio of 10:1; 3) isolate single clones of the resulting cell line; 4) test the response of the isolated clones to Tc dosage to select clones with the highest fold change in GFP signal; 5) establish the Tc dosage curve for the clones selected; 6) test the response of the clones selected to the proteasome inhibitor (MG132) and activators (PSMD11 and PSMD11-S14D) using the Tc concentration resulting in highest sensitivity to changes in UPS activity; 7) verify GFP and tTA protein levels via Western blot.

3.2. Verifying CRISPR-mediated Knockout Controls

One positive control and one negative control were designed to test the efficacy of CRISPR-mediated knockout in cells expressing the *e*Deg-On_2 system. The result of the transduction experiment performed using tTA gRNA virus to knockout tTA from the *e*Deg-On_2 system supported my hypothesis: tTA knockout removed the function of tTA as a regulator in the *e*Deg-On_2 system; as a result, the GFP fluorescence of cells transduced with viruses expressing tTA-specific gRNA was found unchanged upon Tc dosage.

3.3. Titrating CRISPR-mediated Knockout Virus

Different methods for virus titration were proposed: the RNA titration method based on the measurement of viral particles in the supernatant is the most straightforward method, although it may overestimate the real titer by counting in defective viral particles. The DNA titration method is more accurate than the RNA

titration method, and is not limited by the expression of the transgene; however, the choice of the primers to amplify the sequences in the transgene is critical and unspecific binding of the primers in the genome can also lead to overestimation of the titer. The functional titration method is the most accurate method, because the expression of the transgene is the desired output for most experiments.

The virus titration was conducted by quantifying the antibiotic resistance marker gene, and the quantification was performed by counting the number of surviving cells after antibiotic selection to calculate cell viability. The accuracy of quantification of cell viability based on mere counting could be enhanced by including more replicates. Alternatively, the number of viable cells could also be determined by quantifying the concentration of ATP as an indicator of metabolically active cells.

3.4. Mock Screen in HEK293/*e*Deg-On_2 Cells

The robustness of the HEK293/*e*Deg-On_2 cell line was evaluated through two mock screens by either introducing CRISPR-mediated knockouts into cells to induce changes in fluorescence or directly modulating Tc concentrations to tune the fluorescence of cells. In the first mock screen, one negative control and one positive control were mixed at different ratios to mimic the representation of hits in a real screen, and this positive control (tTA knockout) mimics the theoretical strongest proteasome activator that results in maximal degradation of tTA. Tc-induced HEK293/*e*Deg-On_2 cells with different levels of GFP fluorescence were used as

positive controls in the second mock screen, and these positive controls mimic potential proteasome activators of varying strength capable of inducing different levels of GFP fluorescence.

3.5. Validation of Hits from the GeCKOv2 Screen

Identified hits from the GeCKOv2 screen will be first validated through CRISPR-mediated knockout to confirm that the expression of the gene(s) of interest is reduced by the knockout. Selected genes will be verified individually via lentivirus-mediated knockout. Sequence analysis of the endogenous gene will be performed to verify the presence of indel mutations introduced by CRISPR-mediated genome editing, and gene expression will be examined at the transcriptional and the post-translational level by qRT-PCR and Western blot analyses. The influence of individual knockout on the *e*Deg-On_2 system will also be evaluated by monitoring GFP fluorescence of HEK293/*e*Deg-On_2 cells transduced with lentivirus containing gRNA targeting the gene of interest, and comparing with the GFP fluorescence of cells transduced with non-targeting gRNA virus.

Genes selected using the primary screen will be validated through a series of counter screens and secondary assays to confirm their identity as true proteasome activators upon CRISPR-mediated knockout. Individual gene knockouts will be first verified in HEK293/*e*Deg-On_2 cells co-expressing iRFP to confirm that CRISPR-mediated knockout results in increase GFP/iRFP ratio. To verify the function of the genes selected, a series of counter screens and secondary assays will also be

performed. Selected hits will be tested via CRISPR-mediated knockout in the context of: i) the *e*Deg-On system based on wild type TetR without any degron tag to eliminate false positives that may induce increase in GFP fluorescence by downregulating TetR expression or upregulating GFP expression; ii) a direct reporter consisting of GFP fused to a degradation tag (GFP-Deg) to verify that knockout of selected genes induces degradation of tTA-Deg rather than changes in tTA or GFP expression; iii) a GFP-Deg reporter under the control of a signal sequence to direct expression in the secretory pathway (Link et al., 2005) to test whether selected genes affect ERAD in addition to proteasomal degradation; iv) the αsyn-split GFP assay (Kothawala et al., 2012) to quantify changes in aggregation of the misfolding-prone protein α-synuclein and counter select genes that increase GFP output by enhancing protein aggregation.

In summary, I validated the HEK293/*e*Deg-On_2 cell line as a platform to quantify changes in proteasomal degradation. These results will inform the design of CRISPR-mediated whole-genome knockout screens to isolate proteasome regulators, which will open the way to the development of therapeutic approaches for diseases characterizes by accumulation of misfolded proteins.

Chapter 4

Materials and Methods

4.1. Chemicals and Reagents

Tetracycline (Tc) was purchased from Invitrogen. MG-132 was purchased from Fisher Scientific. Zeocin, blasticidin and puromycin were purchased from Invivogen, hygromycin B from Gold Biotechnology and Geneticin (G418) from Sigma-Aldrich.

High-glucose Dulbecco's modified eagle's medium (DMEM) and penicillin streptomycin glutamine (PSQ) were purchased from GE Healthcare, fetal bovine serum (FBS) was from Sigma-Aldrich, PBS was purchased from Lonza, and TrypLE was from Life Technologies. The JetPrime transfection reagents were purchased from Polyplus Transfection.

4.2. Plasmid Construction

The ptTA_2 plasmid was constructed by replacing the puromycin resistance cassette in the ptTA plasmid (Zhao et al., 2014) with the hygromycin resistance cassette using the restriction enzymes PstI and BlpI (New England Biolabs).

The pQTEV-PSMD11 plasmid was purchased from Addgene. The PSMD11 cassette was cloned from the pQTEV-PSMD11 plasmid to the pcDNA3.1+ backbone (Invitrogen) using restriction enzymes BamHI and NotI (New England Biolabs). The S14D mutation was introduced into the PSMD11 gene via site-directed mutagenesis using primers (forward: 5'- AGTTCCAGAGAGCCCAGGACCTACTCAGCACCGACCG-3' and reverse: 5'-CGGTCGGTGCTGAGTAGGTCCTGGGCTCTCTGGAACT-3').

The nontargeting (NT)-, USP14- and tTA-gRNA plasmids were constructed as previously described (Shalem et al, 2014 and Sanjana et al., 2014). Briefly, the gRNAs targeting genes were designed using the online software CRISPR Design (http://crispr.mit.edu/). Paired gRNA oligos (NT: 5'-CACCGACGGAGGCTAAGCGTCGCAA-3' as forward and 5'-CTGCCTCCGATTCGCAGCGTTCAAA-3' as reverse; tTA: 5'-CACCGCTTAATGAGGTCGGAATCGA-3' as forward and 5'-CGAATTACTCCAGCCTTAGCTCAAA-3' as reverse; USP14: CACCGgctcagctgtttgcgttgac-3' as forward and 5'-gtcaacgcaaacagctgagcCAAA-3' as reverse) for each gene were then annealed and cloned into the plentiCRISPRv2 backbone (Addgene) using the restriction enzyme BsmBI (Fermentas).

4.3. Cell Culture and Transfection

Human embryonic kidney cell line 293 (HEK293), HEK293 with SV40 large T antigen stable integration (HEK293T) and HEK293 derived stable cell lines were maintained in high-glucose DMEM medium supplemented with 10% FBS and 1% PSQ, and were passaged every other day at split ratios ranging from 1:6 to 1:12 to prevent cells from reaching 90% confluency. HEK293 derived stable cell lines were cultured in medium supplemented with appropriate antibiotics once in every three passages to ensure the stability of the new cell line.

Cells were transfected using JetPrime transfection reagents according to the manufacturer's protocol. Briefly, cells were plated at 50% confluency 22-26 hours prior to transfection. Cells were supplemented with JetPrime buffer, plasmid DNA, and JetPrime reagent mixtures on the day of transfection, and the medium was replaced 24 hours after transfection.

4.4. HEK293/*e*Deg-On_2 Stable Cell Line Generation

HEK293 cells were transiently transfected with the linearized TO_GFP plasmid (Zhao et al, 2014) and stably transfected cells were selected using medium containing zeocin (150 μg/ml) for 3 weeks. The cells displaying the highest fluorescence (20% of the total population) were selected using fluorescence-activated cell sorting (FACS). The resulting population was transiently transfected with linearized ptTA and pTRE_tTA plasmids at 1:5 ratio. Stably transfected cells

were selected using medium containing hygromycin (200 μg/ml) and blasticidin (3 μg/ml) for 3 weeks. Selected cells were subcultured in 96-well plates to isolate monoclonal populations of HEK293 expressing the *e*Deg-On_2 system (HEK293/*e*Deg-On_2 cells).

4.5. Virus Production, Titration and Transduction

HEK293T cells below passage 10 were plated into T175 flasks (Greiner Bio-one) one day prior to transfection at 60-70% confluency. Cells were transfected with the envelope plasmid (pMD2.g), the packaging plasmid (psPAX2) and the plasmid of interest according to the manufacturer's protocols (Polyplus transfection) at a ratio of 5:7.5:10 in a 20 μg DNA solution. The medium was replaced with fresh medium 7 hours post-transfection and virus was harvested from the medium after 48 hours by filtration using a 0.45 μm filter (EMD Millipore Corp) and concentrated using the LentiX concentrator (Clontech) according to the manufacturer's protocols. Virus was aliquoted and stored at -80 °C.

Virus was titrated as described previously (Sastry et al., 2002). Briefly, the viral RNA was extracted using the ZR Viral RNA Kit (Zymo Research) and converted to cDNA using the QuantiTect Rev. Transcription Kit (Qiagen). The concentration of viral cDNA was determined using quantitative PCR (qPCR).

The MOI was determined as previously described (Shalem et al., 2014). Briefly, cells were plated in 12-well plate at 60% confluency. Cells were transduced

with different volumes of concentrated virus ranging from 0 (control) to 20 μl per well in the presence of 4 μg/ml Polybrene (Sigma-Aldrich) after 24 hours and split into duplicate wells the next day. Cells in one replicate well were selected with 0.5 μg/ml of puromycin while cells in the other well were maintained in medium without puromycin. The volume of virus corresponding to an MOI of 0.2 was determined as the volume of virus corresponding to 20% cell viability upon antibiotic selection.

To transduce HEK293/*e*Deg-on_2 cells with virus expressing the gRNA HEK293/*e*Deg-on_2 cells were plated at 60% confluency one day prior to transduction and transduced with the gRNA virus at an MOI of 0.2 in the presence of 8 μg/ml of Polybrene. Cells were replaced with fresh media 24 hours post-transduction, and stably transduced cells were selected using medium containing 0.5 μg/ml puromycin for 7 days.

4.6. T7EI Analysis

The genomic DNA of cells modified via CRISPR-cas technology was extracted using the E.Z.N.A Tissue DNA Kit according to manufacturer's protocols (Omega Bio-tek). The T7EI assay was performed as previously described (Kim et al., 2009). Briefly, the USP14-modified genomic region was amplified via PCR and gel-purified using the Gel/PCR DNA Fragments Extraction Kit according to manufacturer's protocols (IBI Scientific). A total of 400 ng of purified PCR product was hybridized

and reannealed to allow the formation of heteroduplex DNA using the following PCR cycles: 5min of denaturation at 95 ºC, followed by fast cooling to 85 ºC at -2 ºC /s, and slow cooling to 25 ºC at -0.1 ºC /s. The heteroduplex DNA was incubated with 3 units of T7 Endonuclease I (New England Biolabs) for 45 min and the reaction was terminated by adding 1 μl of 0.25M EDTA per 200 ng of DNA. Signs of T7EI-digested DNA were examined on a 1.5% agarose gel.

4.7. Flow Cytometry Analysis

Cells were analyzed with a FACSCanto II flow cytometer (BD, San Jose, CA) to measure fluorescence intensity of GFP (488 nm laser, 530/30 nm emission filter) and iRFP (640 nm laser, 660/20 emission filter). At least 10,000 cells were recorded in each sample for analysis.

For transient transfection experiments, we monitored changes in GFP signal within iRFP-positive cells to monitor changes in GFP signal within transfected cells. The reported output signal was calculated by normalizing GFP to iRFP signal to eliminate differences arising from transfection efficiencies.

4.8. Quantitative PCR

Quantitative PCR was performed using viral cDNA as template, primers specific for the *cas9* gene in the viral genome (forward: 5'-CGTGACCGAGGGAATGAGAAAGC-3' and reverse: 5'-AGCAGATCGTGGTATGTGCCC-3'),

and PerfeCTa SYBR Green FastMix (Quanta Biosciences) according to manufacturer's protocols. Standards of qPCR were generated via serial dilutions of linearized plentiCRISPR plasmids with known *cas9* copy numbers. PCR reactions were performed using a CFX96 Real-Time PCR Detection System (Bio-Rad) as follows: one cycle of 2 min at 95 °C, followed by 40 cycles of 1s at 95 °C, 30s at 60 °C, and 30s at 72 °C. Result analysis was performed using the CFX Manager software (Bio-Rad).

4.9. Statistical Analyses

Data were presented as arithmetic mean ± standard deviation of at least three biological replicates unless otherwise stated. Statistical significance was determined by the Student's t-test assuming two tails and equal variance.

References

Ahler, E., Sullivan, W., Cass, A., Braas, D., York, A., Bensinger, S., Graeber, T., and Christofk, H. (2013). Doxycycline Alters Metabolism and Proliferation of Human Cell Lines. Plos One 8, e64561.

Bence, Sampat, and Kopito (2001). Impairment of the Ubiquitin-Proteasome System by Protein Aggregation. Science 292, 1552–1555.

Bogyo, M., and Wang, E.W. (2002). Proteasome inhibitors: complex tools for a complex enzyme. Curr. Top. Microbiol. Immunol. *268*, 185–208.

Burger, A., and Seth, A. (2004). The ubiquitin-mediated protein degradation pathway in cancer: therapeutic implications. Eur. J. Cancer *40*, 2217–2229.

Chondrogianni, N., Petropoulos, I., Grimm, S., Georgila, K., Catalgol, B., Friguet, B., Grune, T., and Gonos, E. (2012). Protein damage, repair and proteolysis. Molecular Aspects of Medicine.

Cong, L., Ran, F., Cox, D., Lin, S., Barretto, R., Habib, N., Hsu, P., Wu, X., Jiang, W., Marraffini, L., et al. (2013). Multiplex Genome Engineering Using CRISPR/Cas Systems. Science *339*, 819–823.

Cross, B., Lawo, S., Archer, C., Hunt, J., Yarker, J., Riccombeni, A., Little, A., McCarthy, N., and Moore, J. (2016). Increasing the performance of pooled CRISPR–Cas9 drop-out screening. Sci Reports *6*, 31782.

DeJesus, R., Moretti, F., McAllister, G., Wang, Z., Bergman, P., Liu, S., Frias, E., Alford, J., Reece-Hoyes, J., Lindeman, A., et al. (2016). Functional CRISPR screening identifies the ufmylation pathway as a regulator of SQSTM1/p62. Elife *5*.

Diaz, A., Qin, H., Ramalho-Santos, M., and Song, J. (2015). HiTSelect: a comprehensive tool for high-complexity-pooled screen analysis. Nucleic Acids Res *43*, e16–e16.

Doench, J.G., Fusi, N., Sullender, M., Hegde, M., Vaimberg, E.W., Donovan, K.F., Smith, I., Tothova, Z., Wilen, C., Orchard, R., et al. (2016). Optimized sgRNA design to maximize activity and minimize off-target effects of CRISPR-Cas9. Nat. Biotechnol. 34, 184–191.

Geraerts, M., Willems, S., Baekelandt, V., Debyser, Z., and Gijsbers, R. (2006). Comparison of lentiviral vector titration methods. Bmc Biotechnol 6, 34.

Gilbert, L.A., Larson, M.H., Morsut, L., Liu, Z., Brar, G.A., Torres, S.E., Stern-Ginossar, N., Brandman, O., Whitehead, E.H., Doudna, J.A., et al. (2013). CRISPR-mediated modular RNA-guided regulation of transcription in eukaryotes. Cell 154, 442–451.

Gilon, T., Chomsky, O., and Kulka, R.G. (1998). Degradation signals for ubiquitin system proteolysis in Saccharomyces cerevisiae. EMBO J. 17, 2759–2766.

Glick, B. (1995). Metabolic load and heterologous gene expression. Biotechnol Adv 13, 247–261.

Guerrero, C., Milenković, T., Pržulj, N., Kaiser, P., and Huang, L. (2008). Characterization of the proteasome interaction network using a QTAX-based tag-team strategy and protein interaction network analysis. Proceedings of the National Academy of Sciences *105*, 13333–13338.

Hanna, J., Hathaway, N., Tone, Y., Crosas, B., Elsasser, S., Kirkpatrick, D., Leggett, D., Gygi, S., King, R., and Finley, D. (2006). Deubiquitinating Enzyme Ubp6 Functions Noncatalytically to Delay Proteasomal Degradation. Cell *127*.

Hart, T., Chandrashekhar, M., Aregger, M., Steinhart, Z., Brown, K.R., MacLeod, G., Mis, M., Zimmermann, M., Fradet-Turcotte, A., Sun, S., et al. (2015). High-Resolution CRISPR Screens Reveal Fitness Genes and Genotype-Specific Cancer Liabilities. Cell 163, 1515–1526.

Heckl, D., and Charpentier, E. (2015). Toward Whole-Transcriptome Editing with CRISPR-Cas9. Mol Cell 58, 560–562.

Hu, G., and Luo, J. (2012). A primer on using pooled shRNA libraries for functional genomic screens. Acta Bioch Bioph Sin *44*, 103–112.

Hu, M., Li, P., Song, L., Jeffrey, P.D., Chenova, T.A., Wilkinson, K.D., Cohen, R.E., and Shi, Y. (2005). Structure and mechanisms of the proteasome-associated deubiquitinating enzyme USP14. EMBO J. 24, 3747–3756.

Huang, L., and Chen, C.H. (2009). Proteasome regulators: activators and inhibitors. Current Medicinal Chemistry *16*, 931–939.

Inglese, J., Johnson, R., Simeonov, A., Xia, M., Zheng, W., Austin, C., and Auld, D. (2007). High-throughput screening assays for the identification of chemical probes. Nat Chem Biol 3, 466–479.

Jariel-Encontre, I., Bossis, G., and Piechaczyk, M. (2008). Ubiquitin-independent degradation of proteins by the proteasome. Biochim. Biophys. Acta *1786*, 153–177.

Joung J, Konermann S & Gootenberg JS (2016) Protocol: Genome-scale CRISPR-Cas9 Knockout and Transcriptional Activation Screening. *bioRxiv*. Available at: http://www.biorxiv.org/content/early/2016/06/18/059626.abstract.

Kaake, R., Kao, A., Yu, C., and Huang, L. (2014). Characterizing the Dynamics of Proteasome Complexes by Proteomics Approaches. Antioxidants & Redox Signaling *21*.

Komander, D. (2009). The emerging complexity of protein ubiquitination. Biochem. Soc. Trans *37*, 937.

Konermann, S., Brigham, M., Trevino, A., Joung, J., Abudayyeh, O., Barcena, C., Hsu, P., Habib, N., Gootenberg, J., Nishimasu, H., et al. (2015). Genome-scale transcriptional activation by an engineered CRISPR-Cas9 complex. Nature *517*, 583–588.

Kothawala, A., Kilpatrick, K., Novoa, J.A., and Segatori, L. (2012). Quantitative analysis of alpha-synuclein solubility in living cells using split GFP complementation. PloS one *7*, e43505.

König, R., Chiang, C., Tu, B., Yan, S., DeJesus, P., Romero, A., Bergauer, T., Orth, A., Krueger, U., Zhou, Y., et al. (2007). A probability-based approach for the analysis of large-scale RNAi screens. Nat Methods *4*, 847–849.

Larson, M., Gilbert, L., Wang, X., Lim, W., Weissman, J., and Qi, L. (2013). CRISPR interference (CRISPRi) for sequence-specific control of gene expression. Nat Protoc *8*, 2180–2196.

Lee, B.-H., Lee, M., Park, S., Oh, D.-C., Elsasser, S., Chen, P.-C., Gartner, C., Dimova, N., Hanna, J., Gygi, S., et al. (2010). Enhancement of proteasome activity by a small-molecule inhibitor of USP14. Nature *467*, 179–184.

Li, W., Xu, H., Xiao, T., Cong, L., Love, M., Zhang, F., Irizarry, R., Liu, J., Brown, M., and Liu, X. (2014). MAGeCK enables robust identification of essential genes from genome-scale CRISPR/Cas9 knockout screens. Genome Biol *15*, 554.

Li, X., Zhao, X., Fang, Y., Jiang, X., Duong, T., Fan, C., Huang, C.-C., and Kain, S. (1998). Generation of Destabilized Green Fluorescent Protein as a Transcription Reporter. J. Biol. Chem. *273*, 34970–34975.

Liang, P., Xu, Y., Zhang, X., Ding, C., Huang, R., Zhang, Z., Lv, J., Xie, X., Chen, Y., Li, Y., et al. (2015). CRISPR/Cas9-mediated gene editing in human tripronuclear zygotes. Protein Cell 6, 363–372.

Lin, S., Staahl, B., Alla, R., and Doudna, J. (2014). Enhanced homology-directed human genome engineering by controlled timing of CRISPR/Cas9 delivery. Elife 3.

Link, C., Fonte, V., Hiester, B., Yerg, J., Ferguson, J., Csontos, S., Silverman, M., and Stein, G. (2006). Conversion of Green Fluorescent Protein into a Toxic, Aggregation-prone Protein by C-terminal Addition of a Short Peptide. Journal of Biological Chemistry 281, 1808–1816.

Lokireddy, S., Kukushkin, N., and Goldberg, A. (2015). cAMP-induced phosphorylation of 26S proteasomes on Rpn6/PSMD11 enhances their activity and the degradation of misfolded proteins. Proc Natl Acad Sci*112*, E7176–E7185.

Luo, B., Cheung, H.W., Subramanian, A., Sharifnia, T., Okamoto, M., Yang, X., Hinkle, G., Boehm, J.S., Beroukhim, R., Weir, B.A., et al. (2008). Highly parallel identification of essential genes in cancer cells. Proc. Natl. Acad. Sci. U.S.A. *105*, 20380–20385.

Ma, H., Dang, Y., Wu, Y., Jia, G., Anaya, E., Zhang, J., Abraham, S., Choi, J.-G.G., Shi, G., Qi, L., et al. (2015). A CRISPR-Based Screen Identifies Genes Essential for West-Nile-Virus-Induced Cell Death. Cell Rep 12, 673–683.

Maeder, M., Linder, S., Cascio, V., Fu, Y., Ho, Q., and Joung, J. (2013). CRISPR RNA-guided activation of endogenous human genes. Nat Meth 10, 977–979.

Mali, P., Aach, J., Stranges, P., Esvelt, K., Moosburner, M., Kosuri, S., Yang, L., and Church, G. (2013). CAS9 transcriptional activators for target specificity screening and paired nickases for cooperative genome engineering. Nat Biotechnol *31*, 833–838.

Malina, A., Katigbak, A., Cencic, R., Maïga, R., Robert, F., Miura, H., and Pelletier, J. (2014). Methods in Enzymology.

Metzger, M., Maurer, M., Dancy, B., and Michaelis, S. (2008). Degradation of a Cytosolic Protein Requires Endoplasmic Reticulum-associated Degradation Machinery. Journal of Biological Chemistry 283, 32302–32316.

Nakamura, N., Harada, K., Kato, M., and Hirose, S. (2014). Ubiquitin-specific protease 19 regulates the stability of the E3 ubiquitin ligase MARCH6. Exp Cell Res 328, 207–216.

Nijman, S.M., Luna-Vargas, M.P., Velds, A., Brummelkamp, T.R., Dirac, A.M., Sixma, T.K., and Bernards, R. (2005). A genomic and functional inventory of deubiquitinating enzymes. Cell 123, 773–786.

Oddo, S. (2008). The ubiquitin‐proteasome system in Alzheimer's disease. J. Cell. Mol. Med. *12*, 363–373.

Olanow, C., and McNaught, K. (2006). Ubiquitin–proteasome system and Parkinson's disease. Mov Disord. *21*, 1806–1823.

Pfoh, R., Lacdao, I., and Saridakis, V. (2015). Deubiquitinases and the new therapeutic opportunities offered to cancer. Endocr. Relat. Cancer 22, T35–T54.

Pickering, A., and Davies, K. (2012). Differential roles of proteasome and immunoproteasome regulators Pa28αβ, Pa28γ and Pa200 in the degradation of oxidized proteins. Arch. Biochem. Biophys. *523*, 181–190.

Qi, L., Larson, M., Gilbert, L., Doudna, J., Weissman, J., Arkin, A., and Lim, W. (2013). Repurposing CRISPR as an RNA-Guided Platform for Sequence-Specific Control of Gene Expression. Cell *152*.

Qiu, P., Shandilya, H., D'Alessio, J.M., O'Connor, K., Durocher, J., and Gerard, G.F. (2004). Mutation detection using Surveyor nuclease. BioTechniques 36, 702–707.

Raasi, S., and Wolf, D. (2007). Ubiquitin receptors and ERAD: a network of pathways to the proteasome. Semin. Cell Dev. Biol. *18*, 780–791.

Rechsteiner, M., and Hill, C. (2005). Mobilizing the proteolytic machine: cell biological roles of proteasome activators and inhibitors. Trends in Cell Biology *15*, 2733.

Ren, Q., Li, C., Yuan, P., Cai, C., Zhang, L., Luo, G., and Wei, W. (2015). A Dual-Reporter System for Real-Time Monitoring and High-throughput CRISPR/Cas9 Library Screening of the Hepatitis C Virus. Sci Reports *5*, 8865.

Sander, J., and Joung, J. (2014). CRISPR-Cas systems for editing, regulating and targeting genomes. Nat Biotechnol *32*, 347–355.

Sanjana, N., Shalem, O., and Zhang, F. (2014). Improved vectors and genome-wide libraries for CRISPR screening. Nat Meth *11*, 783–784.

Sastry, L., Johnson, T., Hobson, M., Smucker, B., and Cornetta, K. (2002). Titering lentiviral vectors: comparison of DNA, RNA and marker expression methods. Gene Ther *9*.

Scherr, M., Battmer, K., Blömer, U., Ganser, A., and Grez, M. (2001). Quantitative determination of lentiviral vector particle numbers by real-time PCR. BioTechniques *31*, 520, 522, 524, passim.

Shalem, O., Sanjana, N.E., and Zhang, F. (2015). High-throughput functional genomics using CRISPR-Cas9. Nat. Rev. Genet. 16, 299–311.

Sittampalam GS, Gal-Edd N, Arkin M, et al., editors. Assay Guidance Manual [Internet]. Bethesda (MD): Eli Lilly & Company and the National Center for Advancing Translational Sciences; 2004-. Available from: http://www.ncbi.nlm.nih.gov/books/NBK53196/

Strezoska, Ž., Licon, A., Haimes, J., Spayd, K.J., Patel, K.M., Sullivan, K., Jastrzebski, K., Simpson, K.J., Leake, D., van Brabant Smith, A., et al. (2012). Optimized PCR conditions and increased shRNA fold representation improve reproducibility of pooled shRNA screens. PLoS ONE *7*, e42341.

Timms, R., Menzies, S., Tchasovnikarova, I., Christensen, L., Williamson, J., Antrobus, R., Dougan, G., Ellgaard, L., and Lehner, P. (2016). Genetic dissection of mammalian ERAD through comparative haploid and CRISPR forward genetic screens. Nat Commun *7*, 11786.

Trader, D.J., Simanski, S., Dickson, P., and Kodadek, T. (2017). Establishment of a suite of assays that support the discovery of proteasome stimulators. Biochim. Biophys. Acta 1861, 892–899.

Tzelepis, K., Koike-Yusa, H., De Braekeleer, E., Li, Y., Metzakopian, E., Dovey, O.M., Mupo, A., Grinkevich, V., Li, M., Mazan, M., et al. (2016). A CRISPR Dropout Screen Identifies Genetic Vulnerabilities and Therapeutic Targets in Acute Myeloid Leukemia. Cell Rep 17, 1193–1205.

Vilchez, D., Boyer, L., Morantte, I., Lutz, M., Merkwirth, C., Joyce, D., Spencer, B., Page, L., Masliah, E., Berggren, W., et al. (2012). Increased proteasome activity in human embryonic stem cells is regulated by PSMD11. Nature *489*, 304–308.

Vilchez, D., Morantte, I., Liu, Z., Douglas, P.M., Merkwirth, C., Rodrigues, A.P., Manning, G., and Dillin, A. (2012). RPN-6 determines C. elegans longevity under proteotoxic stress conditions. Nature 489, 263-268.

Wang, X., Yen, J., Kaiser, P., and Huang, L. (2010). Regulation of the 26S Proteasome Complex During Oxidative Stress. Science Signaling *3*, ra88ra88.

Wu, Y., Zhou, L., Wang, X., Lu, J., Zhang, R., Liang, X., Wang, L., Deng, W., Zeng, Y.-X., Huang, H., et al. (2016). A genome-scale CRISPR-Cas9 screening method for protein stability reveals novel regulators of Cdc25A. Cell Discov *2*, 16014.

Yang, H., Wang, H., Shivalila, C.S., Cheng, A.W., Shi, L., and Jaenisch, R. (2013). One-Step Generation of Mice Carrying Reporter and Conditional Alleles by CRISPR/Cas-Mediated Genome Engineering. Cell 154, 1370–1379.

Zavacki, AM, e Drigo, RA, and Freitas, B. (2009). The E3 ubiquitin ligase TEB4 mediates degradation of type 2 iodothyronine deiodinase. … and Cellular Biology.

Zhao, W., Bonem, M., McWhite, C., Silberg, J., and Segatori, L. (2014). Sensitive detection of proteasomal activation using the Deg-On mammalian synthetic gene circuit. Nat Comms *5*, -.

Zhou, Y., Zhu, S., Cai, C., Yuan, P., Li, C., Huang, Y., and Wei, W. (2014). High-throughput screening of a CRISPR/Cas9 library for functional genomics in human cells. Nature *509*, 487–491.